Supporting Information

Washington et al. 10.1073/pnas.1606322113

SI Materials and Methods

Alignment and Phylogenetic Tree. All finished, permanent draft, and draft genomes on the IMG database (40) were searched for HopAF1 homologs using blastp (87) with *Pto* DC3000 HopAF1 as a query. The resulting 180 matches were aligned using MUSCLE (88) with default parameters. The alignment revealed that many of the HopAF1 genes were annotated with a truncated ORF. Therefore, longer alternative ORFs were selected manually for all truncated genes and were trimmed to the correct size after realignment to the nontruncated sequences. Following realignment, sequences that did not contain the putative catalytic region were discarded, resulting in 166 protein sequences from 143 genomes. The putative catalytic positions D154, C159, and H186 were conserved in all these sequences. A phylogenetic tree was constructed using a maximum likelihood method based on the JTT matrix-based model (89). The bootstrap consensus tree inferred from 1,000 replicates was taken to represent the evolutionary history of the analyzed sequences (90). Initial tree(s) for the heuristic search were obtained by applying the neighbor-joining method to a matrix of pairwise distances estimated using a JTT model. Evolutionary analyses were conducted in MEGA6 (91).

The phylogenetic history of Pseudomonads and Xanthomonads was inferred by concatenating and aligning 23 single-copy conserved clusters of orthologous groups (COGs) for the largest subset of HopAF1-containing genomes that had all 23 COGs (91 *Pseudomonas* and 27 *Xanthomonas* genomes; all excluded genomes had highly related neighbors that were included). Phylogenetic trees were constructed as described above. Trees were visualized using iTOL (itol.embl.de/) (92).

Transient Expression of AvrXv3 in Tomato. The coding sequences of AvrXv3 and AvrXv3$_{H126A}$ were cloned in the binary Gateway vector, pGWB17, which carries a C-terminal 4x-myc tag. Triparental mating was used to transfer this construct to *Agrobacterium* strain C58C1. For transient expression of AvrXv3 in tomato plants, the strains expressing AvrXv3 variants were grown overnight in LB medium at 28 °C. The bacteria were centrifuged at 6,800 × *g* for 5 min and were resuspended in 10 mM $MgCl_2$ at an OD of 0.1. Fully expanded leaves were infiltrated with the bacterial strains and maintained in the greenhouse for 48 h (immunoblot samples) or 72 h (HR). Immunoblot analysis of protein samples was completed as described in *Materials and Methods* in the main text.

Cell Fractionations. Two hundred milligrams of tissue was flash-frozen in liquid nitrogen and ground in sucrose buffer [20 mM Tris·HCl (pH 8.0), 0.33M sucrose, 1 mM EDTA (pH 8.0), 5 mM DTT, one cOmplete protease inhibitor tablet per 50 mL buffer l (Roche)]. The homogenate was centrifuged for 10 min at 2,000 × *g* at 4 °C. The supernatant was collected as the total fraction. A portion of the total fraction was spun again for 30 min at 20,000 × *g* at 4 °C. The supernatant from this spin was collected as the soluble fraction. The pellet, which became the microsomal fraction, was resuspended in equal volumes of the sucrose buffer described above.

MTN1 Purification. MTN1 (At4g38800) and the noted variants were purified as previously described (58). In brief, a PreScission Protease cleavage site was cloned onto the N terminus of MTN1, which then was cloned into the Gateway vector pDEST15, which carries an N-terminal GST tag. This clone was transformed into Novagen Rosetta *E. coli* BL21(DE3) cells. A 5-mL overnight culture was used to inoculate 1 L of LB medium containing 100 μg/mL ampicillin. Cells were grown at 37 °C to an OD of 0.6–0.8. The temperature was reduced to 22 °C. Protein production was induced with 1 mM isopropyl β-D-1-thiogalactopyranoside (IPTG), and cells continued to grow at 22 °C overnight. MTN1 was purified with a GST affinity purification step followed by PreScission Protease cleavage and reverse chromatography to isolate "free" MTN1 in the flowthrough fractions.

HopAF1 Purification. N-terminal 6xHis affinity tag constructs for HopAF1 and HopAF1$_{H186A}$ were generated by ligation independent cloning (93). 6xHisMBP-Δ130HopAF1 and 6xHisMBP-Δ147HopAF1 were generated by cloning a tobacco etch virus (TEV) protease cleavage site onto the N terminus of the truncated HopAF1 ORFs and cloning them into the Gateway-compatible pDEST-HisMBP vector. All HopAF1 bacterial expression constructs were transformed into ArticExpress (DE3)RIL (Agilent) cells. To initiate protein production, overnight cultures were used to inoculate 5 L of LB medium containing 100 μg/mL ampicillin at a 1:200 dilution. Cells were grown at 28 °C until the OD reached 0.6–0.8; then the temperature was reduced to 14 °C. Protein production was induced with 1 mM IPTG, and cells continued to grow overnight at 14 °C.

Purification of 6xHis-HopAF1 and 6xHis-HopAF1$_{H186A}$ involved affinity purification on a HisTrap column (GE Healthcare) followed by additional purification with the HiPrep 16/60 Sephacryl S-200 High Resolution size-exclusion column (GE Healthcare). The HopAF1 fractions that were not in the void volume were collected for in vitro assays.

Purification of 6xHisMBP-Δ130HopAF1 and 6xHisMBP-Δ147HopAF1 also began with a His affinity purification followed by dialysis into TEV cleavage buffer [20 mM Tris (pH 8.0), 50 mM NaCl, 1 mM DTT, and 0.5 mM EDTA] and TEV cleavage at room temperature for 6 h. Reverse affinity chromatography was used to collect the HopAF1 truncations into relatively pure fractions. These fractions were dialyzed into anion exchange buffer [20 mM Tris (pH 8.0), 50 mM NaCl] overnight at 4 °C and further purified with the anion exchange HiLoad 16/10 Q Sepharose column (GE Healthcare). Size-exclusion chromatography using a HiPrep 16/60 Sephacryl S-200 High Resolution column resulted in monodispersed protein.

Circular Dichroism. 6xHis-HopAF1, 6xHis-HopAF1$_{H186A}$, and MTN1 were purified as previously described and dialyzed into a buffer containing 20 mM sodium phosphate (pH 7.4) and 150 mM NaF. Samples of ~0.4 mg/mL (HopAF1 variants) or 0.5 mg/mL (MTN1) were placed in a 1.0-mm cuvette. Molar ellipticity measurements were collected at 25 °C from 185–260 nm on a Chirascan-plus CD spectrometer (Applied Photophysics, Ltd.).

Induction of Native Promoter HopAF1 in Minimal Medium. Genomic clones of wild-type HopAF1, HopAF1$_{H186A}$, and HopAF1$_{G2AC4S}$, including the native promoter with a *hrp*-box, were cloned into a Gateway-compatible vector, pJC531, carrying a C-terminal HA-tag. This clone was transformed into *P. fluorescens*, a strain engineered to express the type III secretion system (63). Strains were spread onto King's media B plates, incubated overnight, and resuspended in minimal medium (7.8 mM ammonium sulfate, 50 mM potassium phosphate, 1.7 mM sodium chloride, 1.7 mM NaCl, and 10 mM mannitol) at an OD of 0.02. After growth in 28 °C for 12 h, 2 mL of each culture was centrifuged at room temperature for 5 min at 8,600 × *g*. The pellet was

resuspended in 100 μL of 6x SDS loading buffer and boiled for 10 min; then 10 μL was loaded onto SDS/PAGE gel.

Generating the *mtn1 mtn2* Double Mutant and Complementation Lines. To generate the *mtn1 mtn2* double mutant, which is sterile (65), we obtained and genotyped the previously described GABI Kat lines *mtn1-2* and *mtn2-2* (65). We crossed *mtn1-2* and *mtn2-2*, selfed the resulting T1s, and screened the T2s for lines that were homozygous for *mtn1* and segregating *mtn2*. We maintained several stocks of these lines, which we sowed out and PCR genotyped to identify double homozygous plants at the time of experimentation. Complementation lines were generated by cloning the coding sequence of wild-type MTN1 and variant MTN1s into the UBQ10 promoter Gateway-compatible vector (86). Floral dips of *mtn1* homozygous and *mtn2* heterozygous plants were performed using *Agrobacterium* GV3101 carrying the UBQ10:MTN1 constructs. Transgenes were selected by resistance to Basta and then were genotyped to identify lines in the double homozygous background.

Translocation Assay. Genomic HopAF1 constructs were cloned into pJC532, a Gateway-compatible vector carrying a C-terminal tag of the C-terminal 177 residues of the T3E protein AvrRpt2, from which the N-terminal 79 amino acids of AvrRpt2 were deleted (‘79AvrRpt2) (34, 64). HopAF1-Δ79AvrRpt2, $HopAF1_{H186A}$-Δ79AvrRpt2, and $HopAF1_{G2AC4S}$-Δ79AvrRpt2 were transferred into *Pfo*-1 using triparental mating. Eight leaves of *Arabidopsis* Col-0 were hand-infiltrated per strain, and the HR was scored 24 h post inoculation.

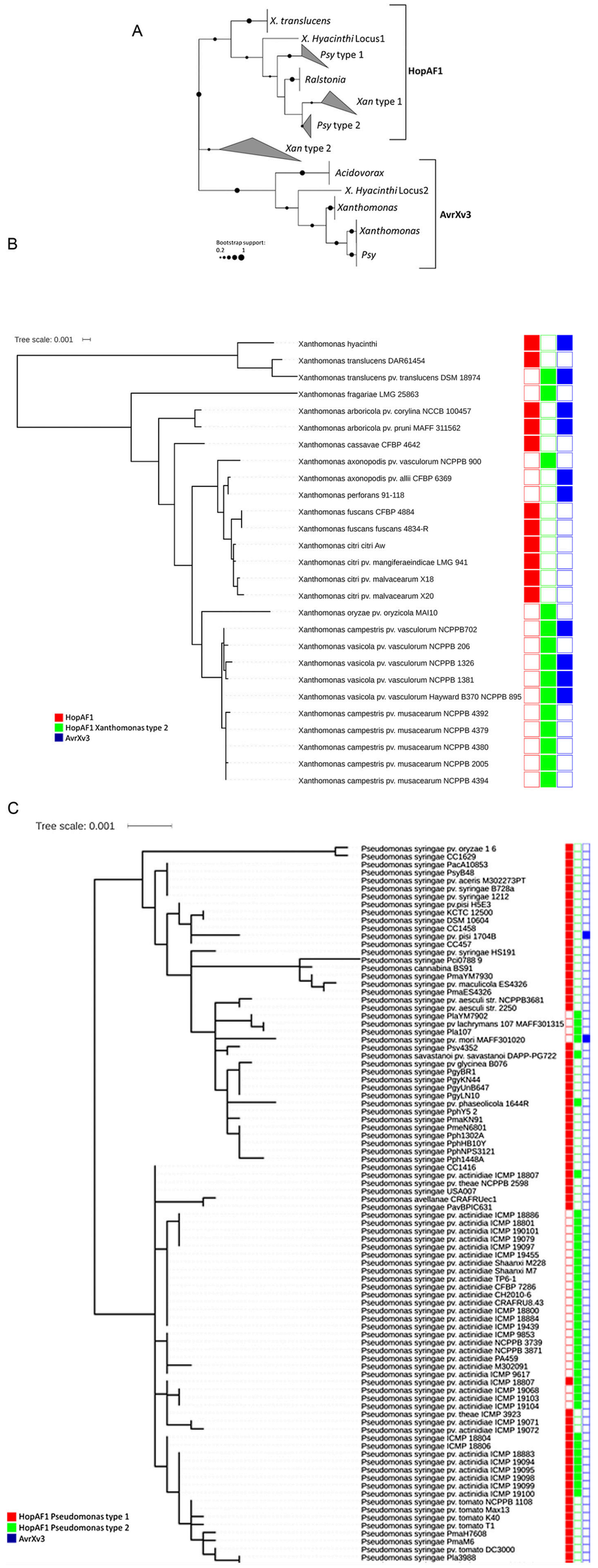

Fig. S1. The HopAF1 evolutionary tree. (*A*) Phylogenetic reconstruction of HopAF1 homologous protein sequences in sequenced genomes. Monophyletic groups belonging to the same genus are collapsed. Sequences cluster into three distinct groups: HopAF1, AvrXv3, and *Xanthomonas* type 2. In cases where two copies are present in the same genome, the text LOCUS 1/2 is appended to the species name. Nodes with bootstrap support >0.2 are marked. The size of the dot is proportional to the level of support. The uncollapsed tree can be viewed on iTOL (itol.embl.de/shared/HopAF1Evo). (*B*) Occurrence of HopAF1/AvrXv3 across the *Xanthomonas* phylogeny. Phylogenetic reconstruction of HopAF1-containing *Xanthomonas*, using a concatenated alignment of 23 single-copy marker genes. The occurrence of the HopAF1 variant and AvrXv3 is marked on the right. Marker genes used for tree construction are the same used for the *P. syringae* tree in *C*. (*C*) The occurrence of HopAF1/AvrXv3 across the *P. syringae* phylogeny. Phylogenetic reconstruction of *P. syringae*, using a concatenated alignment of 23 single copy marker genes. The occurrence of the HopAF1 variant and AvrXv3 is marked on the right. Marker genes used for tree construction were COG0012, COG0016, COG0048, COG0049, COG0052, COG0080, COG0081, COG0087, COG0088, COG0090, COG0091, COG0092, COG0093, COG0094, COG0096, COG0098, COG0102, COG0103, COG0185, COG0186, COG0201, COG0256, and COG0541. All three trees are available for browsing at itol.embl.de/shared/HopAF1Evo.

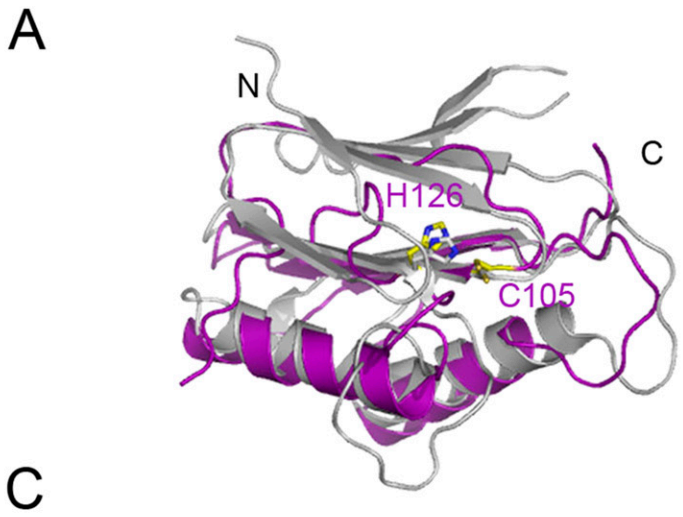

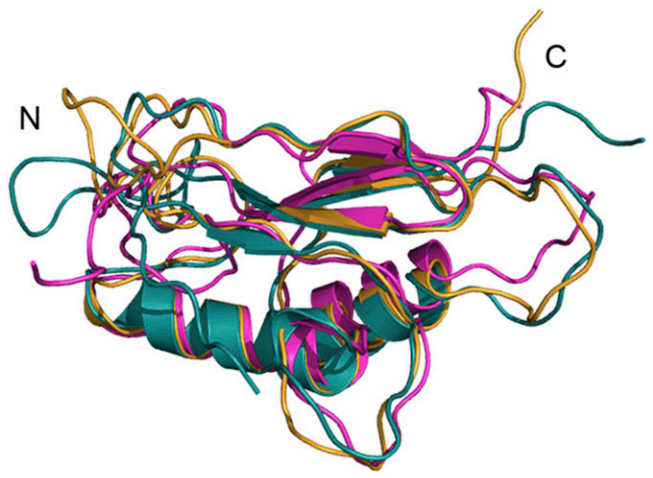

C

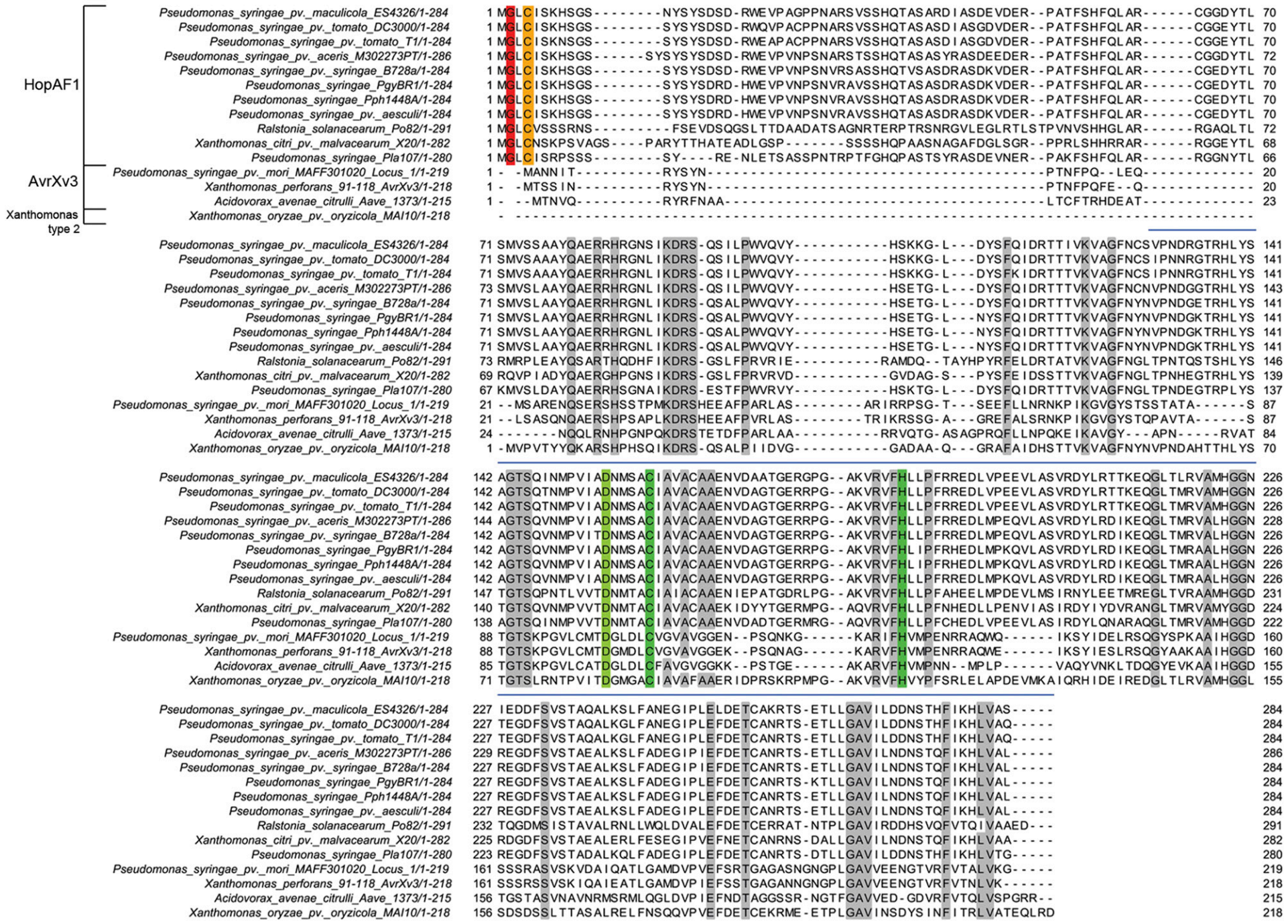

Fig. S2. The HopAF1 protein family. (*A*) Homology model of AvrXv3 from *Xanthomonas vesicatoria* (purple) aligned with CheD (silver). Putative catalytic residues of AvrXv3, C105, and H126, are highlighted in yellow and align with the catalytic residues of CheD (silver line above sequences). (*B*) Independent homology models for additional HopAF1 family members: *P. syringae* pv. *maculicola* ES4326 (HopAF1 type 1; pink), *Xanthomonas oryzae* pv. *oryzicola* MAI10 (*Xanthomonas* type 2; dark teal), and *P. syringae* pv. *lachrymans* pla107 (HopAF1 type 2; orange). (*C*) Representative protein sequences from all major groups of HopAF1 were aligned using VectorNTI AlignX. Amino acids with 80% identity are shaded in gray. Invariant putative catalytic residues are highlighted in dark green, and the conserved aspartic acid is highlighted in light green. Sites of likely posttranslocation myristoylation and palmitoylation are denoted in red and orange, respectively. In the residues underlined in blue represent the putative catalytic domain. Structural images were generated with PyMOL.

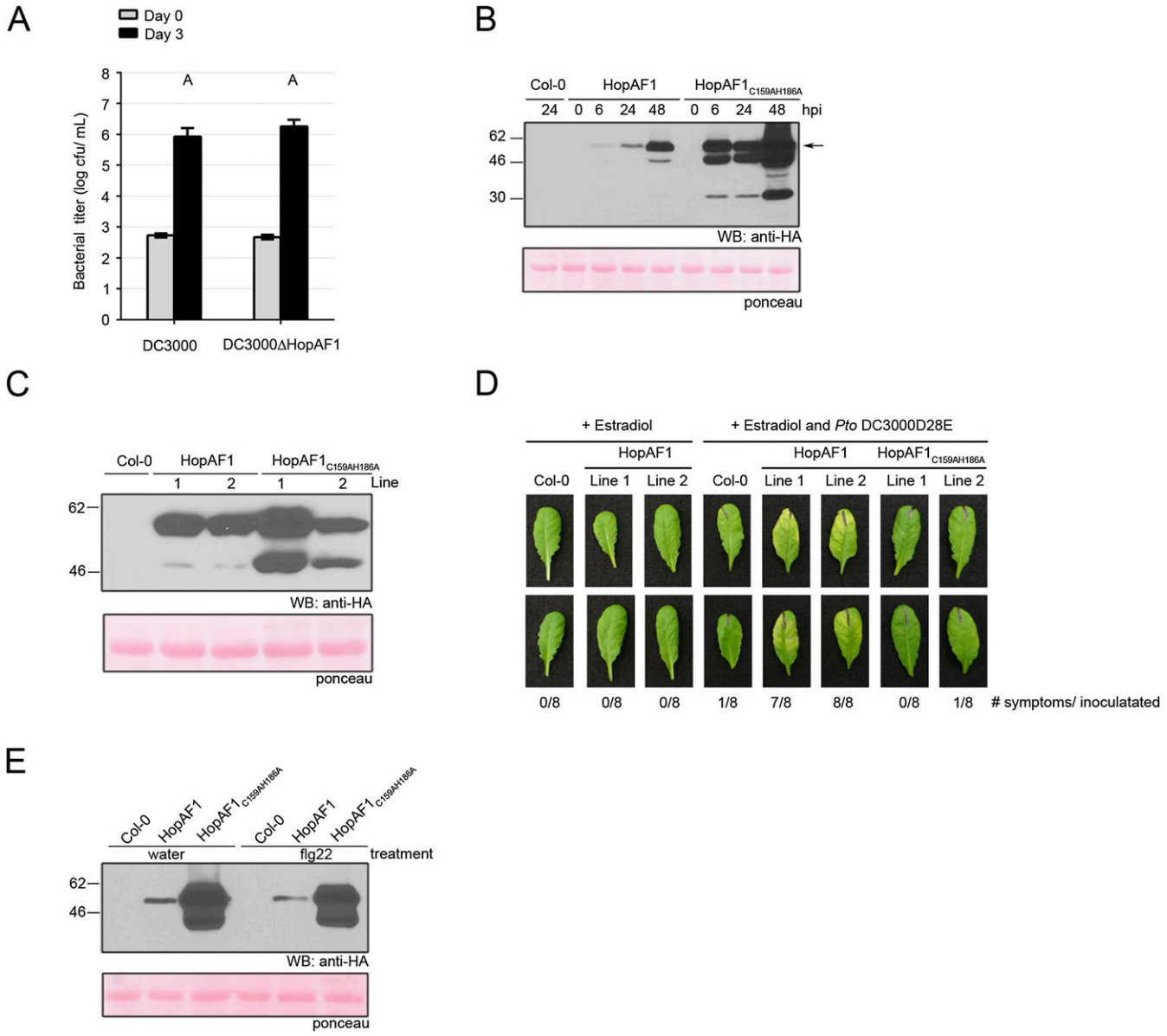

Fig. S3. Protein expression and disease symptoms in HopAF1 transgenic lines. (*A*) Bacterial growth of *Pto* DC3000 and *Pto* DC3000Δ*hopAF1* (46) in Col-0 was measured 0 and 3 d after hand-infiltration with bacteria (1×10^5 cfu/mL). Error bars represent SEM. An ANOVA was performed among the day 3 samples, followed by Tukey's post hoc analysis ($P < 0.05$) denoted by A. (*B*) Immunoblot analysis with anti-HA shows a time course of the expression of HopAF1-cerulean-HA and HopAF1$_{C159AH186A}$-cerulean-HA in transgenic plants after spray application of 20 μM estradiol. (*C*) Immunoblot analysis with anti-HA shows the expression of HopAF1-cerulean-HA and HopAF1$_{C159AH186A}$-cerulean-HA in transgenic plants used in the experiment in Fig. 1*B*. Expression was determined 3 d after spray application of 20 μM estradiol. (*D*) Disease symptoms in Col-0 and two independent lines of HopAF1-cerulean-HA and HopAF1$_{C159AH186A}$-cerulean-HA were photographed 3 d after hand-infiltration with 1×10^5 cfu/mL of *P. syringae* pv. *tomato* DC3000D28E. HopAF1 was induced with the application of 20 μM estradiol 24 h before bacterial inoculation. Numbers below the images denote the ratio of the number of leaves that displayed chlorotic symptoms to the number of leaves inoculated. (*E*) Immunoblot analysis with anti-HA shows the expression of HopAF1-cerulean-HA and HopAF1$_{C159AH186A}$-cerulean-HA in the transgenic plants used in the experiment in Fig. 1*C*. Expression was determined 3 d after bacterial infiltration, which corresponds to 108 h (4.5 d) after estradiol induction.

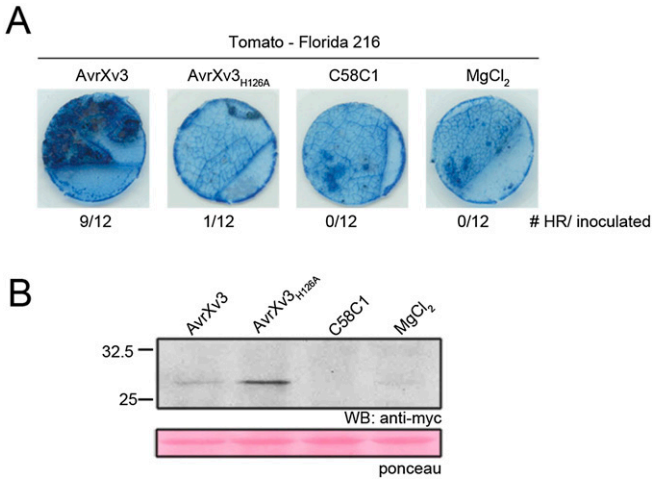

Fig. S4. AvrXv3 putative catalytic residues are required for the HR in tomato. (*A*) AvrXv3-4x myc and AvrXv3$_{H126A}$-4x myc were transiently expressed in tomato cultivar Fla 216 using the *Agrobacterium* strain C58C1. Cores containing both infiltrated and uninfiltrated tissue were removed from the tomato leaves 3 d postinfiltration, and trypan blue staining was used to highlight the cell-death response associated with the HR. Numbers below the images denote the ratio of the number of leaves that displayed the HR to the number of leaves inoculated. (*B*) Anti-myc immunoblot analysis demonstrates the expression of AvrXv3-4x-myc and AvrXv3$_{H126A}$-4x-myc in tomato cultivar Fla 216 3 d postinfiltration. Ponceau staining of the membrane indicates equal loading.

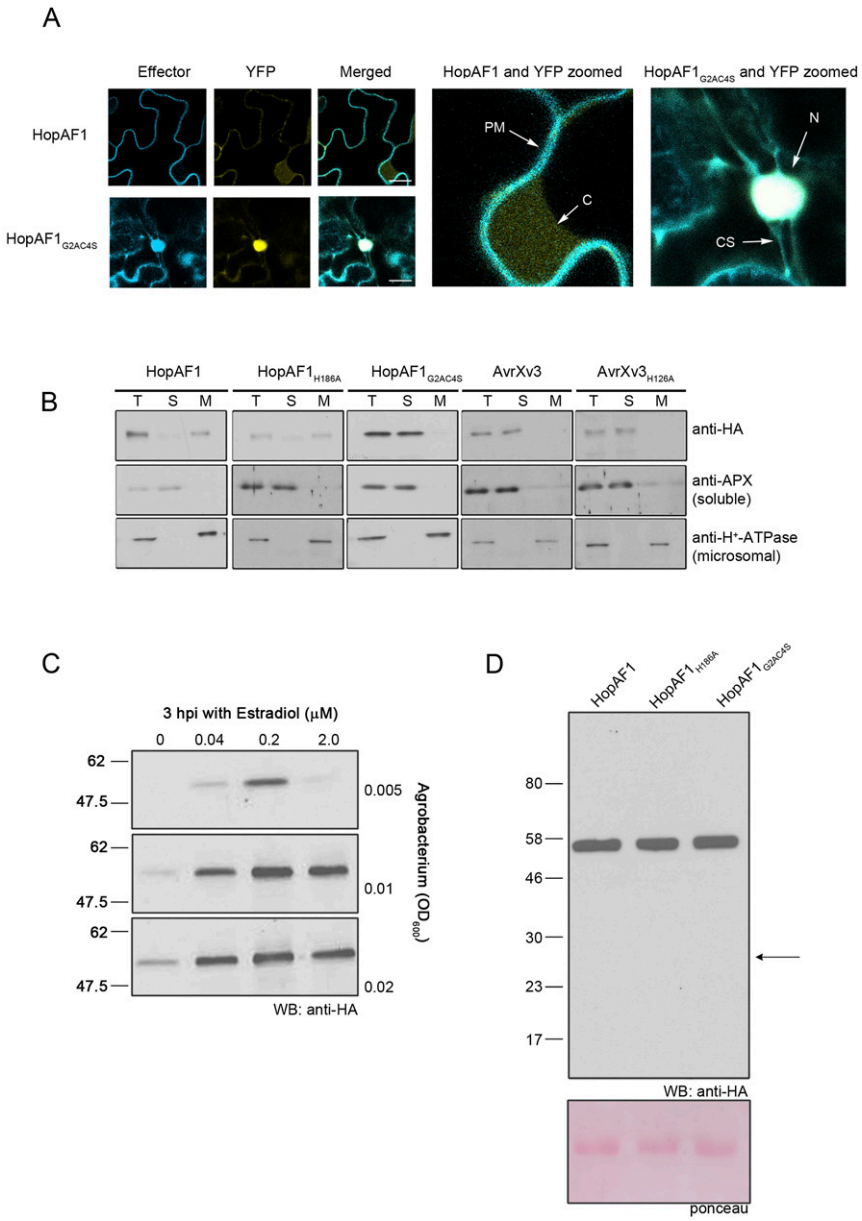

Fig. S5. HopAF1 is targeted to the plasma membrane via acylation. (*A*) The localization of transiently expressed HopAF1-cerulean-HA and HopAF1$_{G2AC4S}$-cerulean-HA was determined with scanning confocal laser microscopy 3 h after estradiol induction in *N. benthamiana* epidermal cells. Free YFP is a soluble protein and therefore can be used as a marker of the plant cytoplasm. White arrowheads indicate the plasma membrane (PM), cytoplasmic streaming (CS) and nuclei (N). (Scale bars, 20 μM.) (*B*) As in Fig. 2, estradiol-inducible HopAF1-cerulean-HA, HopAF1$_{G2AC4S}$-cerulean-HA, HopAF1$_{H186A}$-cerulean-HA, AvrXv3-cerulean-HA, and AvrXv3$_{H126A}$-cerulean HA were expressed transiently in *N. benthamiana* using *Agrobacterium*-mediated transient transformations. Transgene expression was induced with 5 μM estradiol 3 d after bacterial infiltration. The localization of transiently expressed proteins was determined with scanning confocal laser microscopy 3 h after estradiol induction in *N. benthamiana* epidermal cells. Cellular fractionations into total (T), soluble (S), and microsomal (M) fractions were performed. Equal cell equivalents were loaded onto SDS/PAGE gels followed by anti-HA immunoblots to detect the fractions with the expressed proteins of interest. Anti-APX and anti–H^+-ATPase were included as controls for the soluble (S) and microsomal (M) fractions, respectively. (*C*) Levels of HopAF1-cerulean-HA transiently expressed in *N. benthamiana* were titrated by varying the concentration of estradiol and the OD of *Agrobacterium*. Immunoblots with anti-HA were used to detect the expression of HopAF1-cerulean-HA. *N. benthamiana* leaves were sprayed with estradiol 3 d postinfiltration with *Agrobacterium*, and leaf samples were collected 3 h after estradiol application for immunoblot analysis. (*D*) Immunoblot analysis with anti-HA shows the expression of full-length HopAF1-cerulean-HA, HopAF1$_{H186A}$-cerulean-HA, and HopAF1$_{G2AC4S}$-cerulean-HA and the absence of free cerulean (black arrow) at ~27 kDa. As above, *N. benthamiana* leaves were sprayed with 5 μM estradiol 3 d postinfiltration with *Agrobacterium*, and protein samples were collected 3 h after estradiol application. Ponceau staining indicates equal loading. The absence of free cerulean under these conditions indicates that the mislocalized HopAF1 detected in the nucleocytoplasm is not free cerulean diffusing into the nucleus.

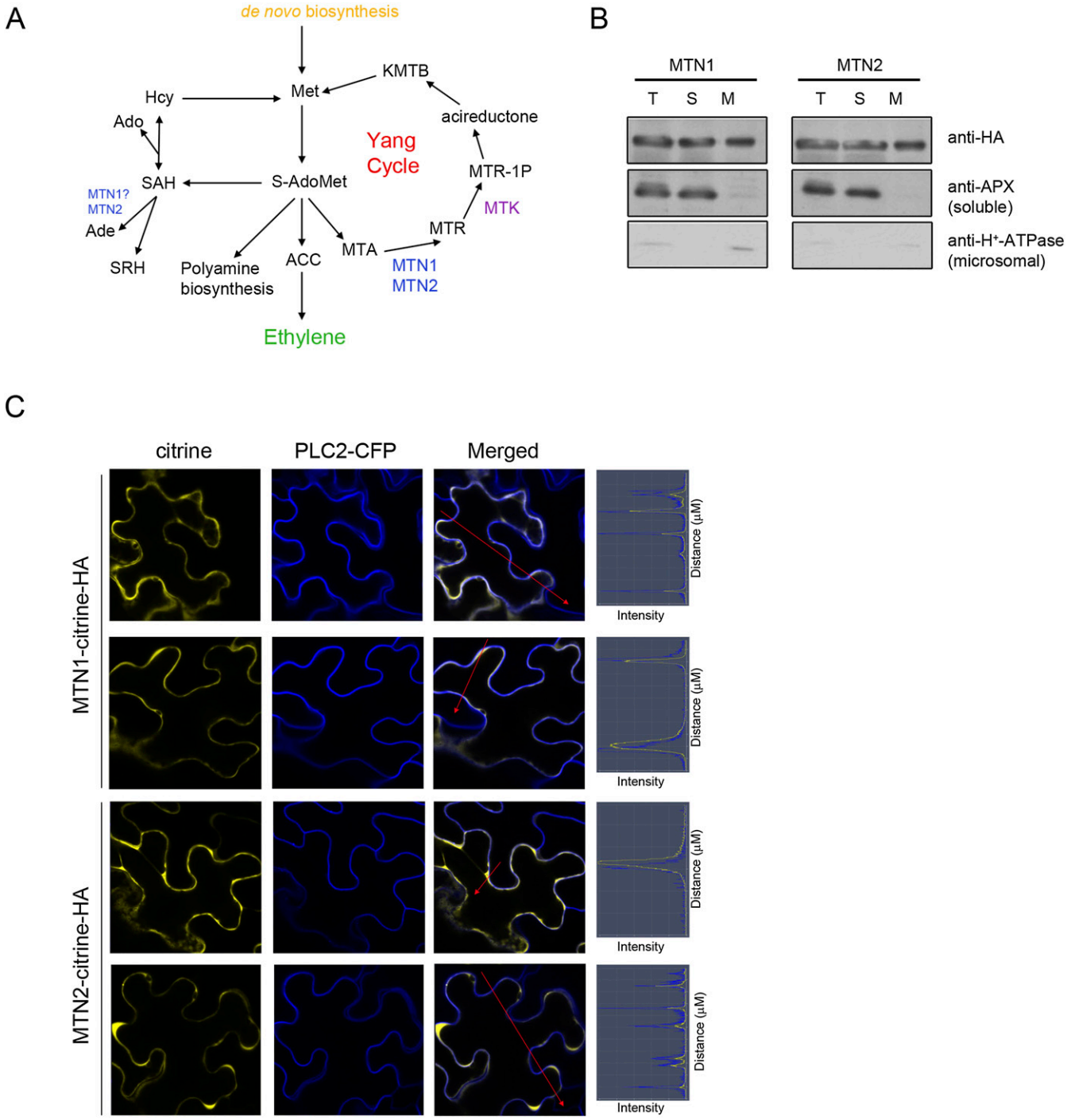

Fig. S6. The Yang cycle proteins MTN1 and MTN2 are found in both the plasma membrane and the cytoplasm. (*A*) In this figure adapted from Rzewuski et al. (94), the relationship between the Yang cycle (also known as the methionine recycling cycle) and the phytohormone ethylene in *Arabidopsis* is highlighted. *Arabidopsis* MTN1 and MTN2 are Yang cycle proteins that can cleave their substrate MTA, resulting in adenine and 5-methylthioribose (MTR) production. MTR then is phosphorylated by the kinase MTK. MTNs also function in a secondary pathway to recycle methionine. Both MTN1 and MTN2 can bind S-adenosylhomocysteine (SAH), but, perhaps as a result of steric hindrance and the rigidity of the ligand-binding pocket of MTN1 (95), only MTN2 has been shown to cleave SAH (71, 95). However, both MTN1 and MTN2 cleave MTA more efficiently than SAH (71). Methionine is a precursor for the ethylene biosynthesis pathway. It is important to note that methionine recycling supplements the continual de novo synthesis of methionine. (*B*) 35S:MTN1-HA and 35S:MTN2-HA were expressed transiently in *N. benthamiana* using *Agrobacterium*-mediated transient transformations. Cellular fractionations into total (T), soluble (S), and microsomal (M) fractions were performed. Equal cell equivalents were loaded onto SDS/PAGE gels followed by anti-HA immunoblots to detect the fractions with the expressed proteins of interest. Anti-APX and anti–H^+-ATPase were included as controls for the soluble (S) and microsomal (M) fractions, respectively. (*C*) Estradiol-inducible MTN1-cerulean-HA and MTN2-cerulean-HA were transiently coexpressed with PLC2-CFP, a plasma membrane marker, in *N. benthamiana* and were imaged using confocal microscopy. The path of the red arrow in the merged images is reflected in the histograms, which display the intensity of citrine and the CFP signal by yellow and blue lines, respectively.

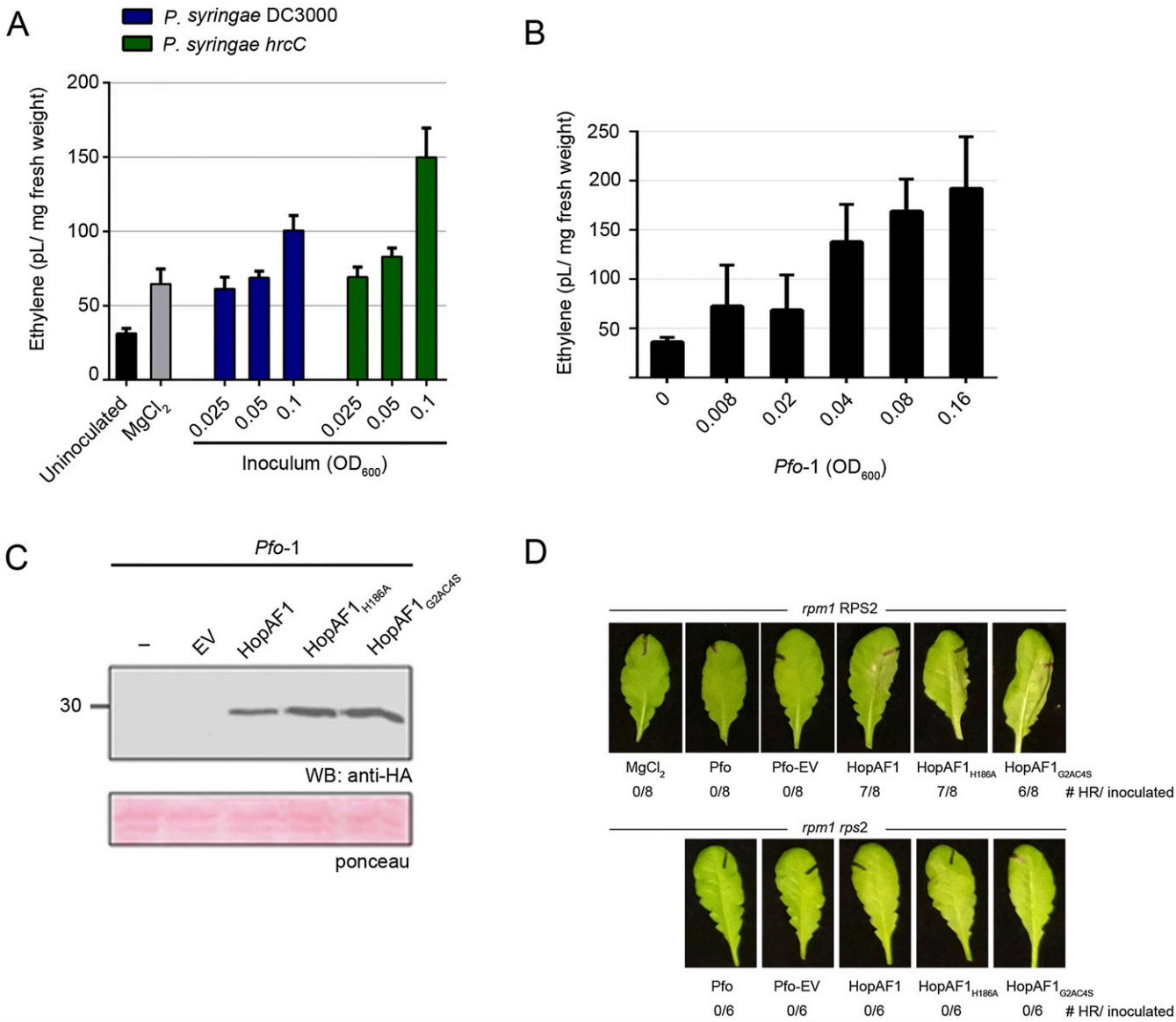

Fig. S7. Establishing *P. fluorescens* as a tool to determine the effect of HopAF1 on PAMP-induced ethylene accumulation. (*A*) *Arabidopsis* leaves were hand-infiltrated with multiple concentrations of *Pto* DC3000 and *Pto* DC3000 *hrcC* (a type III secretion system-deficient mutant). The fresh weight of four leaves was measured 3 h postinfiltration; then these leaves were sealed in a vial for 24 h before ethylene accumulation was measured using gas chromatography. An ANOVA was performed, followed by Tukey's post hoc analysis ($P < 0.05$); error bars represent SE. (*B*) The histogram demonstrates the increase in ethylene biosynthesis elicited by increasing concentrations of *Pfo*-1. (*C*) Immunoblot analysis of HA-tagged HopAF1 variants expressed in *Pfo*-1 strains induced with minimal medium for 12 h. Protein was detected with anti-HA monoclonal antibody. (*D*) AvrRpt2 translocation assay to monitor HopAF1 translocation into plant cells. Col-0 *rpm1 RPS2* leaves were inoculated with *Pfo-1* expressing HopAF1 variants fused to the Δ79AvrRpt2 reporter (HopAF1-Δ79AvrRpt2, HopAF1$_{H186A}$-Δ79AvrRpt2, and HopAF1$_{G2AC4S}$-Δ79AvrRpt2) and were observed after 24 h. The ability to elicit an AvrRpt2-dependent HR in the *RPS2* background, as indicated by tissue collapse, is evidence of the translocation of the fusion proteins. The ratio of the number of leaves in which the HR was evident to the number of leaves inoculated is displayed below the representative leaves for each *Pfo-1* inoculation. There was no HR in the *rpm1 rps2* background.

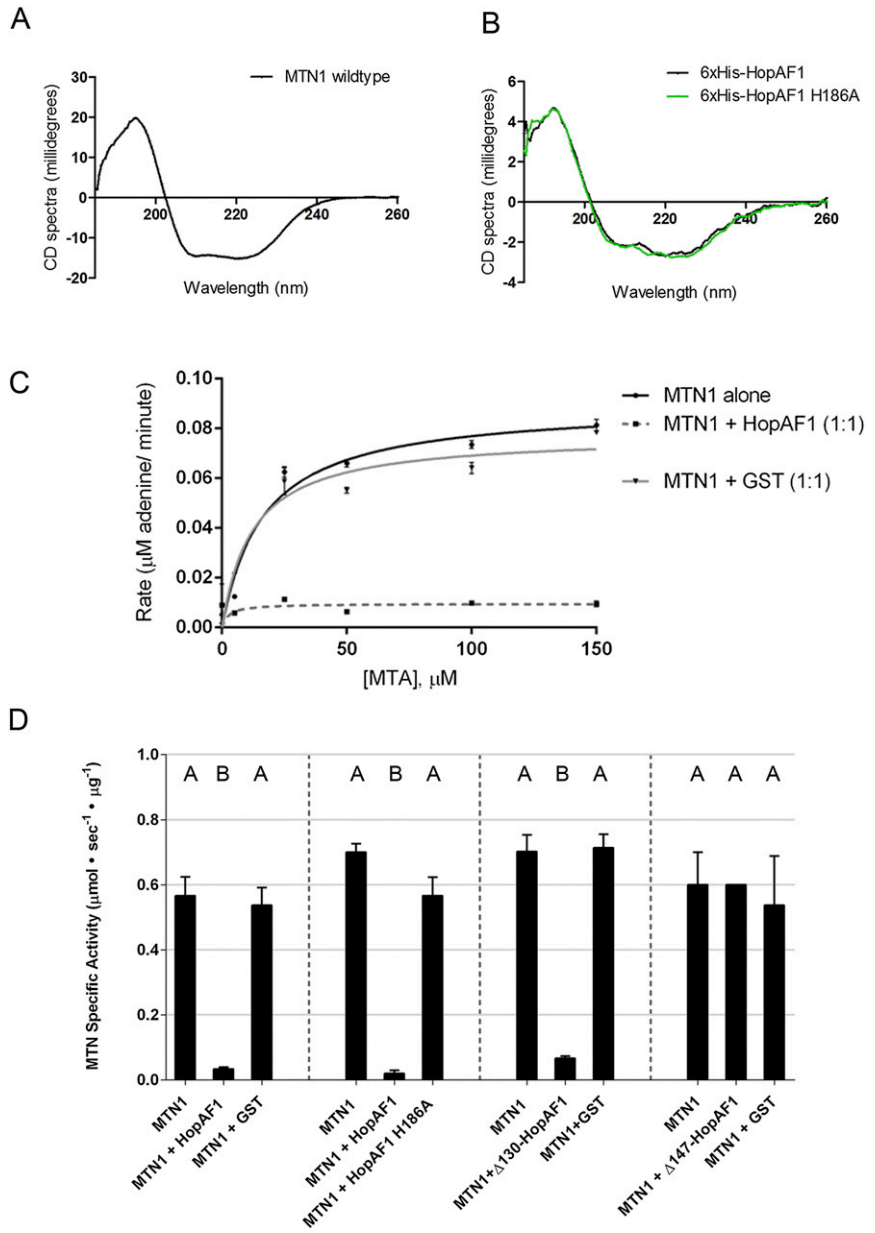

Fig. S8. HopAF1 inhibition of MTN1 activity in vitro is dependent on catalytic activity. (*A* and *B*) Circular dichroism spectra collected at 25 °C at the far-UV CD spectrum (185–260 nm) demonstrates that wild-type MTN1, 6xHis-HopAF1, and 6xHis-HopAF1$_{H186A}$ have a secondary structure. The H186A mutation in HopAF1 does not perturb the secondary structure. The buffer control [20 mM sodium phosphate (pH 7.4), 150 nM NaF] was set as the baseline and was subtracted from the protein-associated spectra above. (*C*) Michaelis–Menten plot of MTN1 activity measured in vitro using a xanthine oxidase-coupled spectrometric assay. Recombinant MTN1 was incubated for 18 h in buffer at 37 °C alone or with equimolar amounts of recombinant wild-type 6xHis-HopAF1 or GST. (*D*) MTN1 enzyme-specific activity measured in vitro using a xanthine oxidase-coupled spectrometric assay. MTN1 was incubated at 37 °C for 18 h with equimolar amounts of 6xHis-HopAF1, 6xHis-HopAF1 H186A, Δ147-HopAF1, Δ130-HopAF1, and GST. An ANOVA was performed, followed by Tukey's post hoc analysis ($P < 0.05$). Error bars represent SE. Different letters indicate groups that differ significantly.

A

```
ATHALIANA1/1-267          1 -MAPHGDGLSDIEEPEVDAQSEIL-RPISSVVFVIAMQAEALPLVNKFGLSETTDSPLGKGLPWVLYHGVH 69
ATHALIANA2/1-254          1 ---------------MEGVMGQVEKRPISTIVFIVAMQKEAQPLINRLRLVEEVNTPFPKEVTWIMFKGMY 56
BNAPUS_(EST)/1-205        1 -MGPHGDG--DIENVE--SESRR--RPISTVVFVIATQAEAQPLVNKFGLSETSDSPLGKGLPWVLYHGLH 64
OSATIVA/1-259             1 ----------MAPPSDSDDSAPIPAGAISKLLIVIAMQTEALPLVNKFHLVEAEESIFPKGAPWIRYHGNY 61
SLYCOPERSICUM_(EST)/1-258 1 MAPPHGDKSAEVKEEAAAAVSSVDNRPISTILFIVAMQTEALPLVKKFQLTEDLNSVFPKGVPWVRFYGNY 71
VVINIFERA/1-268           1 ----MAPHDDRSDVAEEAMVAEAEKRPIATIVIIIAMQTEALPLVNRFQLTEDLDSVFPRGVPWVRYHGIY 67
ECOLI/1-232               1 ----------------------------MKIGIIGAMEEEVTLLRDKIENRQTISLGG-----CEIYTGQL 38
                                                                        N113

ATHALIANA1/1-267         70 KDLRINVVCPGRDAALGIDSVGTVPASLITFASIQALKPDIIINAGTCGGFKVKGANIGDVFLVSDVVFHD 140
ATHALIANA2/1-254         57 KDLNINIVCPGKDSTLGVESVGTVPASLVTYASILAIQPDLIINAGTAGGFKAKGACISDVYVVSTVAFHD 127
BNAPUS_(EST)/1-205       65 KDLRIYVVCPGKDAASGIDSVGTVPASLITFASIQALQPDILINAGTCGAFKVKGANIGDVFLVSDVVFHD 135
OSATIVA/1-259            62 KGLHVDLVWPGKDPVLGVDCVGTVSAALVTYASIQSLKPDLIINAGTAGGFKAKGADTGDVYLASDVAFHD 132
SLYCOPERSICUM_(EST)/1-258 72 KGLTVNIVCPGKDPALGVDGVGTVSASLVTYASVQALKPDLIINAGTAGGFGAKGASIGDVFISSEVAFHD 142
VVINIFERA/1-268          68 KDLHISIIWPGKDLVLGVDNVGTVSASFVTYASIQALQPDLVINAGTAGGFKAKGACVGDVVLATDVAFHD 138
ECOLI/1-232              39 NGTEVALLKSG---------IGKVAAALGATLLLEHCKPDVIINTGSAGGLAPT-LKVGDIVVSDEARYHD 99
                                                  N169                  N194

ATHALIANA1/1-267        141 RR-IPIP----MFDLYGVGLRQ----AFSTPNLLKELNLK--IGRLSTGDSLDMSTQDETLIIAN--DATL 198
ATHALIANA2/1-254        128 RR-IPVP----VLDIYGVGMRN----TFPTPNLIKELNLK--VGRLSTGDSMDMSPHDEESITAN--DATV 185
BNAPUS_(EST)/1-205      136 RRRIPIP----MFDLYGVGLRQ----AFSTPNLLKELNLK--IGRLSTGDSLDMSTQDESLIIAN--DATL 194
OSATIVA/1-259           133 RR-IPIP----VFDMYGIGTRK----TFATPNILKELNLK--VGKLSTGDSLDMSPHDESAILNN--DATV 190
SLYCOPERSICUM_(EST)/1-258 143 RR-IPIP----VFDIYGVGSRK----AFATPNLLKELNLK--VGKLSTGDSLDMSPMDEASIIAN--DATI 200
VVINIFERA/1-268         139 RR-IPIPFLLQVFDQYGIGLRK----ACSAPNLLKELNL---IGALSTGDSLDMSPHDESSILAN--GATV 199
ECOLI/1-232             100 ADVTAFGYEYGQLPGCPAGFKADDKLIAAAEACIAELNLNAVRGLIVSGDAFINGSVGLAKIRHNFPQAIA 170

ATHALIANA1/1-267        199 KDMEGAAVAYVADLLKIPVVFLKAVTDLVDGD-KPTAEEFLQNLTVVTAALEGTATKVINFINGRNLSDL 267
ATHALIANA2/1-254        186 KDMEGAAVAYVADIFKVPTILIKGVTDIVDGN-RPTSEEFLENLAAVTAKLDESLTKVIDFISGKCLSDL 254
BNAPUS_(EST)/1-205      195 KDMEGAAVAYV---------------------------------------------------------- 205
OSATIVA/1-259           191 KDMEGAAVAYVADMFSTPAIFVKAVTDIVDGE-KPTAEEFLQNLVAVTAALDKAVTEVVDFISGKCISDL 259
SLYCOPERSICUM_(EST)/1-258 201 KDMEGAAVAYVADLLKVPAIFVKAVTDIVDGD-KPTPEEFLENLVAVTAALDQTATXVV---------- 258
VVINIFERA/1-268         200 KDMEGAAVAYVADLLKVPVIFIKAVTDIVDGE-KPTAEEFLQNLAAVTAALDQSVTKVVDFINGKCISEL 268
ECOLI/1-232             171 VEMEATAIAHVCHNFNVPFVVVRAISDVADQQSHLSFDEFLAVAAKQSSLMVESLVQKLAHG-------- 232
```

B

Fig. S9. In vitro and *in planta* consequences of mutating conserved MTN asparagines. (*A*) Alignment of methylthioadenosine nucleosidase amino acid sequences from plants and *E. coli*. The conserved putative targets of deamidation, N113, N194, and N169, are highlighted in red. (*B*) UBQ:MTN1$_{N113V}$ complementation lines in the *mtn1 mtn2* mutant background show a range of phenotypes in the T1 stage.

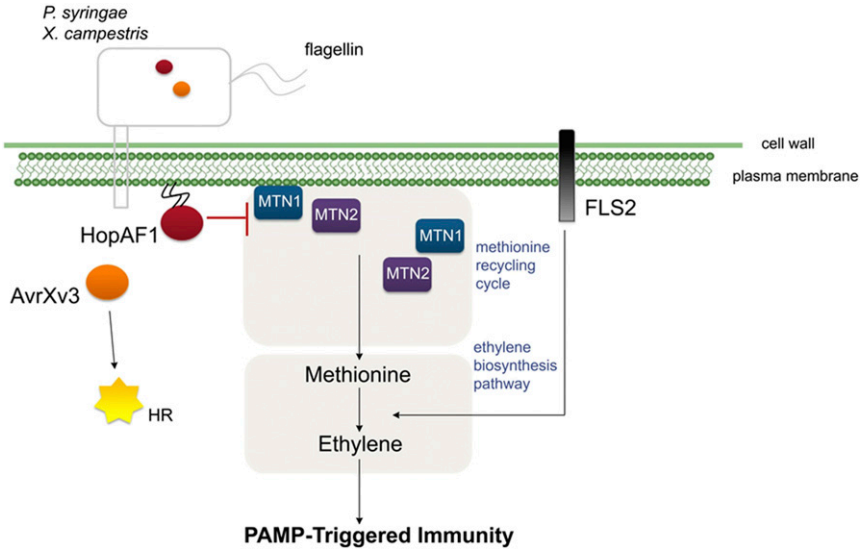

Fig. S10. Working model of *P. syringae* HopAF1 function. Plant pathogens such as *P. syringae* and *X. campestris* deliver multiple T3E proteins into plant cells, including HopAF1 and AvrXv3, respectively. Recognition of PAMPs, such as flg22, a peptide derived from bacterial flagellin, by PRRs such as FLS2 triggers a signal cascade that results in multiple outputs, collectively termed PTI. Through perception of PAMPs, such as flg22, and activation of a MAPK cascade, PTI leads to an increase in ethylene biosynthesis. Our data suggest that HopAF1 inhibits PTI. Our data are consistent with the model that HopAF1 is targeted to the plant plasma membrane via acylation, where it inhibits the function of the Yang cycle proteins MTN1 and MTN2, which are required for the induced level of ethylene that occurs during PTI. As a result, the induced amount of ethylene that occurs during PTI may be an important output, making the Yang cycle an important component of the plant defense pathway and HopAF1 a critical T3E that prevents high ethylene accumulation during the plant defense response by targeting the Yang cycle. Furthermore, we have identified two asparagines in *Arabidopsis* MTN1 and MTN2 that are potential targets of HopAF1-mediated deamidation. Further research is required to determine whether HopAF1 deamidates or modifies *Arabidopsis* MTNs or itself.